# Quantitative Determination of $^1\Sigma_g^+$ and $^1\Delta_g$ Singlet Oxygen in Solvents of Very Different Polarity. General Energy Gap Law for Rate Constants of Electronic Energy Transfer to and from $O_2$ in the Absence of Charge Transfer Interactions

**Reinhard Schmidt***

*Institut für Physikalische und Theoretische Chemie, J. W. Goethe-Universität, Marie-Curie-Str.11, D60439 Frankfurt am Main, Germany*

*Received: November 24, 2005*

The quenching of excited triplet states of sufficient energy by $O_2$ leads to $O_2(^1\Sigma_g^+)$ and $O_2(^1\Delta_g)$ singlet oxygen and $O_2(^3\Sigma_g^-)$ ground-state oxygen as well. The present work investigates the question whether in the absence of charge transfer (CT) interactions between triplet sensitizer and $O_2$ the rate constants of formation of the three different $O_2$ product states follow a generally valid energy gap law. For that purpose, lifetimes of the upper excited $O_2(^1\Sigma_g^+)$ have been determined in a mixture of 7 vol % benzene in carbon tetrachloride, in chloroform, and in perdeuterated acetonitrile. They amount to 1.86, 1.40, and 0.58 ns, respectively. Furthermore, rate constants of $O_2(^1\Sigma_g^+)$, $O_2(^1\Delta_g)$, and $O_2(^3\Sigma_g^-)$ formation have been measured in these three solvents for five $\pi\pi^*$ triplet sensitizers with negligible CT interactions. The rate constants are independent of solvent polarity. After normalization for the multiplicity of the respective $O_2$ product state, the rate constants follow a common dependence on the excess energies of the respective product channels. This empirical energy gap relation describes also quantitatively the rate constants of quenching of $O_2(^1\Delta_g)$ by 28 carotenoids. Therefore, it represents in the absence of CT interactions a generally valid energy gap law for the rate constants of electronic energy transfer to and from $O_2$.

## Introduction

$O_2(^1\Delta_g)$ singlet oxygen is an extremely reactive and highly cytotoxic species, which induces natural photodegradation processes and has significant applications in organic synthesis and in photodynamic therapy.[1−4] The easiest and in fact most important way of $O_2(^1\Delta_g)$ production is its photosensitization via excited triplet ($T_1$) states. Both lowest excited singlet states, $^1\Sigma_g^+$ and $^1\Delta_g$, of $O_2$ of respective energies $E_\Sigma = 157$ and $E_\Delta = 94$ kJ mol$^{-1}$ are competitively formed if the $T_1$ state energy exceeds $E_\Sigma$. The upper excited $O_2(^1\Sigma_g^+)$ is, however, very rapidly and quantitatively deactivated in solution to the long-lived $O_2(^1\Delta_g)$,[5,6] which is commonly being referred to as singlet oxygen.

Both the rate constant $k_T^Q$ of $T_1$ state quenching by $O_2$ and the efficiency $S_\Delta$ of overall $O_2(^1\Delta_g)$ formation depend strongly on the sensitizer triplet-state energy $E_T$,[7] on the sensitizer oxidation potential $E_{OX}$,[8−16] and on the polarity of the solvent.[12,14] A better understanding of the influence of the variation of $E_T$ and $E_{OX}$ on the processes competing in the $T_1$ state quenching by $O_2$ was achieved, when we introduced the separate determination of the three rate constants $k_T^{1\Sigma}$, $k_T^{1\Delta}$, and $k_T^{3\Sigma}$ of $O_2(^1\Sigma_g^+)$, $O_2(^1\Delta_g)$, and $O_2(^3\Sigma_g^-)$ formation.[17] This has been done only in $CCl_4$, where the $O_2(^1\Sigma_g^+)$ lifetime is with $\tau_\Sigma = 130$ ns[18−20] long enough to allow for the quantitative measurement of $O_2(^1\Sigma_g^+)$ via its emissions at 1935 nm (b → a) and 765 nm (b → X), respectively. Using these new techniques, we found in systematic studies with aromatic $T_1(\pi\pi^*)$ sensitizers of widely varying values of $E_T$ and of $E_{OX}$ that the strength of charge transfer (CT) interactions between $T_1$ excited sensitizer and $O_2$ in the initially formed excited $^{1,3,5}(T_1{}^3\Sigma)$ encounter complexes of singlet, triplet, and quintet multiplicity determines the balance of deactivation between a non-CT (nCT) and a CT pathway; see Scheme 1.[21−25]

The strength of CT interactions can be quantified by value of the free energy change $\Delta G_{CET}$ for complete electron transfer from the $T_1$-excited sensitizer to $O_2$ calculated according to the Rehm−Weller equation (eq 1)[26]

$$\Delta G_{CET} = F(E_{OX} - E_{RED}) - E_T + C \qquad (1)$$

where $F$ is the Faraday constant and $E_{RED}$ the reduction potential of $O_2$ (−0.78 V vs SCE in acetonitrile).[27] $C$ is the electrostatic interaction energy which has arbitrarily been set to zero for the solvent $CCl_4$. CT interactions are negligible for sensitizers for which eq 1 results in $\Delta G_{CET} \geq 50$ kJ mol$^{-1}$. In that case, deactivation proceeds only via the nCT deactivation channel, where the rate constants of $O_2(^1\Sigma_g^+)$, $O_2(^1\Delta_g)$, and $O_2(^3\Sigma_g^-)$ formation follow a common dependence on the respective excess energy $\Delta E$ and thus a common dependence on $E_T$.[17,21−23] $\Delta E$ is given by $E_T - 157$, $E_T - 94$, and $E_T$, respectively (in kJ mol$^{-1}$). Reducing $\Delta G_{CET}$ significantly opens the door to an additional second deactivation path, the CT deactivation channel, and leads to an increase of the rate constants of $O_2(^1\Sigma_g^+)$, $O_2(^1\Delta_g)$, and $O_2(^3\Sigma_g^-)$ formation which exponentially depends on $\Delta G_{CET}$. Thus, rather simple relations determine the nCT and CT deactivation paths in the overall sensitization of singlet oxygen by $\pi\pi^*$ excited triplets, which could be used to quantitatively describe the change of the experimental rate constants of $O_2(^1\Sigma_g^+)$, $O_2(^1\Delta_g)$, and $O_2(^3\Sigma_g^-)$ formation in dependence of two variables: $E_T$ and $\Delta G_{CET}$.[24]

This simple two-channel deactivation model rests on data collected only in $CCl_4$. However, as was shown by the

* To whom correspondence should be addressed. Fax: (+49)69-798-29709. E-mail: r.schmidt@chemie.uni-frankfurt.de.

10.1021/jp0568172 CCC: $33.50 
Published on Web 02/08/2006

**SCHEME 1**

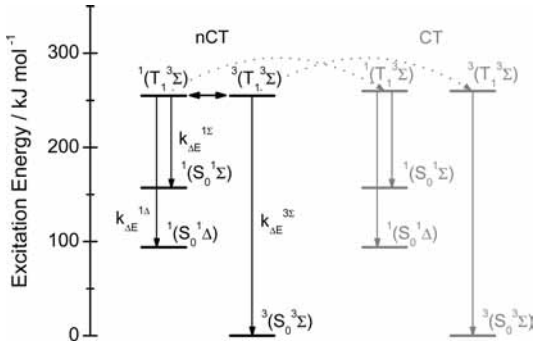


Wilkinson group, variation of the solvent polarity may strongly influence the rate constants and efficiencies of singlet oxygen sensitization.[12,14] Although it seems as if the main effect of the solvent polarity variation concerns CT induced processes, it is still unclear whether the energy gap relation of the rate constants of $O_2(^1\Sigma_g^+)$, $O_2(^1\Delta_g)$, and $O_2(^3\Sigma_g^-)$ formation in the nCT deactivation channel could also be affected. The combination of the generally small b → a and b → X radiative transition probabilities with the very short $O_2(^1\Sigma_g^+)$ lifetimes in other than in perchlorinated solvents prevented hitherto solvent dependent quantitative determinations of $O_2(^1\Sigma_g^+)$.[1] However, recent development of highly amplified semiconductor detectors for the NIR allows at least for integral measurement of the b → a emission at 1935 nm in liquids where $\tau_\Sigma$ is even as low as 1 ns. The mixture of 7 vol % $C_6H_6$ in $CCl_4$ (TET/B) falls with $\tau_\Sigma \approx$ 1.9 ns in that region.[23] $CHCl_3$ and $CD_3CN$, for which we estimate from previously determined rate constants of $O_2(^1\Sigma_g^+)$ quenching respective lifetimes $\tau_\Sigma$ of 1.2 and 0.6 ns should be suited as well.[6] Since these three liquids offer a strongly graduated polarity scale, we choose them for the present investigation of the question, whether solvent polarity influences the energy gap relation of the rate constants of $O_2(^1\Sigma_g^+)$, $O_2(^1\Delta_g)$, and $O_2(^3\Sigma_g^-)$ formation of nCT sensitizers.

## Experimental Section

Phenalenone (PHE, Aldrich, 97%) was purified by column chromatography ($CH_2Cl_2$/silica gel), quinoxaline (QUI, Aldrich, 99%) by vacuum sublimation. Chloranil (CLA, Janssen Chimica, 99%), duroquinone (DQU, Fluka), and 9-bromoanthracene (BRA, Aldrich, 98%) have been crystallized twice, and 2-acetonaphthone (ANA Aldrich, 99%) was used as received. The liquids $CCl_4$ (TET, Merck, Uvasol), $C_6H_6$ (B, Merck p.a.), $CHCl_3$ (Aldrich, 99.8%+ spectrophotometric grade, containing amylene as stabilizer), and $CD_3CN$ (Deutero, 99%) have been used as supplied. Humidity strongly reduces the $O_2(^1\Sigma_g^+)$ lifetime which amounts to $\tau_\Sigma$ = 130 ns in dry pure TET. However, because of the already rather short lifetimes $\tau_\Sigma$ in TET/B, $CD_3CN$, and $CHCl_3$, no particular precautions against humidity had to be taken during the preparation of the solutions. The principal experimental setup was described and is only briefly given here.[28] A Nd:YAG laser (Brilliant) from Quantel with frequency tripling (4 ns, 355 nm) was used to excite the sensitizer solutions, which were optically matched for absorbances of 1.2 per cm at 355 nm. Laser pulse energies were measured deflecting a small portion of the laser beam onto a fast Si diode as detector. Transmission filters attenuated the laser in energy dependent measurements. The setup allowed the simultaneous time-resolved measurement of $O_2(^1\Delta_g)$ via the a → X phosphorescence at 1275 nm (right angle) and the integral detection of $O_2(^1\Sigma_g^+)$ via the b → a fluorescence at 1935 nm (in-line). The following filter/detector combinations have been used: (1) interference filter IF 1275 (hw = 40 nm) and fast liquid-$N_2$ cooled Ge diode with integrated preamplifier (North Coast EO 817P) and (2) IF 1940 nm (hw = 70 nm) plus GG10 filter and liquid $N_2$-cooled InGaAs diode with built in preamplifier (Hamamatsu 7754-01, sensitivity $1.9 \times 10^9$ V/W, NEP $2.5 \times 10^{-14}$ W Hz$^{-0.5}$). The extremely high sensitivity of the new 7754-01 detector to NIR radiation had to be paid by an undesired sensitivity to acoustic waves. Therefore, sound-absorbing material was used to reduce the perturbations originating mainly from the laser cooling unit and from noise of the surrounding laboratories. The time-response of Ge detector and preamplifier was recorded monitoring the fluorescence of erythrosin B (fluorescence lifetime in water 78 ps).[29] This transient signal served as apparatus function AF(t) for the deconvolution of the time-resolved $O_2(^1\Delta_g)$ measurements. The three different signals were intermediately stored by two transient digitizers (Gould 4072) and transferred to a PC for averaging (up to 128 times) and evaluation. $O_2$ concentrations of air-saturated solutions were calculated as $[O_2] = 0.21(p_A - p_V) \times [O_2]_{p=1}$ with $p_A$ and $p_V$ being atmospheric and vapor pressure, and $[O_2]_{p=1}$ is the $O_2$ concentration of the solvent at 1 bar $O_2$ partial pressure. The experimental temperatures (around 25 °C) were measured for evaluation of $p_V$. We take $[O_2]_{p=1}$ = 0.0124 M (TET) and 0.0116 M ($CHCl_3$) listed by Murov et al.[30] $[O_2]_{p=1}$ = 0.0091 M ($CH_3CN$) also given in ref 30 comes from ref 31. Since no original citation is given there, this value has been disregarded. Instead, we assume $[O_2]$ = 0.00242 M determined recently for air-saturated $CH_3CN$ to be valid also for $CD_3CN$.[32]

**TABLE 1: Triplet Quantum Yields $Q_T$, Triplet Energies $E_T$, Oxidation Potentials $E_{OX}$, and Reaction Free Enthalpies $\Delta G_{CET}$ of Complete Electron Transfer from $T_1$ Excited Sensitizer to $O_2$ for Different $\pi\pi^*$ Triplet Sensitizers**

| sensitizer | $Q_T$ | $E_T$, kJ mol$^{-1}$ | $E_{OX}$, V vs SCE | $\Delta G_{CET}$, kJ mol$^{-1}$ |
|---|---|---|---|---|
| PHE | 1.00[a] | 186[e] | 1.96[f] | 78 |
| BRA | 0.99[b] | 168[e] | 1.41[f] | 43 |
| QUI | 0.99[c] | 255[c] | 2.41[g] | 52 |
| ANA | 0.90[d] | 248[e] | 2.01[f] | 21 |
| CLA | 0.98[c] | 266[c] | 2.86[g] | 85 |

[a] Reference 33. [b] Reference 34. [c] Reference 30. [d] Average of $Q_T$ = 0.84 of ref 35 and $Q_T$ = 0.95 of ref 17. [e] Reference 17. [f] Experimental value, $CH_3CN$, ref 24. [g] Extrapolated value, $CH_3CN$, ref 24.

## Results and Discussion

**Quantum Yields $Q_\Sigma$ and $Q_\Delta$ of $O_2(^1\Sigma_g^+)$ and Overall $O_2(^1\Delta_g)$ Sensitization.** CT interactions are negligible for triplet sensitizers with $\Delta G_{CET} \geq 50$ kJ mol$^{-1}$.[24] Table 1 lists the sensitizers used in the present study.

They have been selected since they have large quantum yields $Q_T$ and show a wide variation of triplet energies and oxidation potentials high enough that they can be expected to behave as typical nCT sensitizers. Only ANA has a $\Delta G_{CET}$ value significantly lower than the above given limit. Therefore, CT interactions might become important in polar solvents for ANA.

Figure 1 illustrates the rise of the $I_{1275}(t)$ emission signal of $O_2(^1\Delta_g)$ sensitized by BRA in $CD_3CN$. Equation 2 gives the overall time dependence of $I_{1275}(t)$ on the different variables

$$I_{1275}(t) = c_{1275} n_{1275}{}^{-2} F_{355} Q_\Delta k_{a-X}^{SOL} E_P \{\exp(-t/\tau_\Delta) - \exp(-t/\tau_T)\} \tau_\Delta/(\tau_\Delta - \tau_T) \quad (2)$$

where $c_{1275}$ is the apparatus constant for 1275 nm emission, $n_{1275}$ the respective solvent refractive index, $F_{355}$ is the geometric

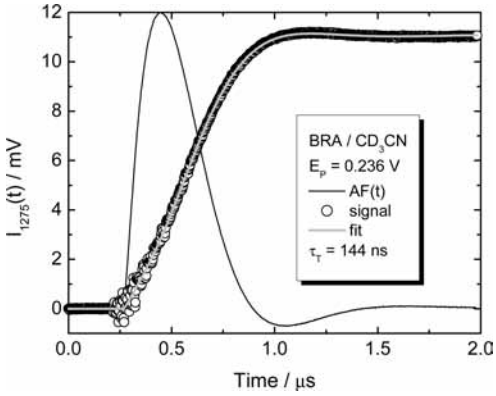


**Figure 1.** Experimental rise of the a → X emission of $O_2(^1\Delta_g)$ at 1275 nm sensitized by BRA in $CD_3CN$ and corresponding fit. AF($t$) is the apparatus function.

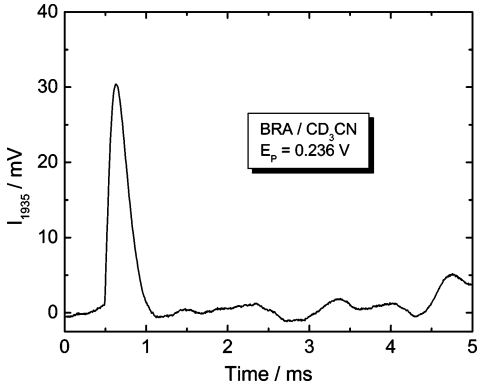


**Figure 2.** b → a emission signal of $O_2(^1\Sigma_g^+)$ at 1935 nm sensitized by BRA in $CD_3CN$.

factor for right angle observation, accounting for the spatial distribution of the emission in the fluorescence cell which depends on the sample absorbance at the laser wavelength, $k_{a-X}^{SOL}$ is the solvent dependent rate constant of the radiative a → X transition, $E_P$ is the laser pulse energy, and $\tau_T$ and $\tau_\Delta$ are the lifetimes of the sensitzer triplet state and of $O_2(^1\Delta_g)$.

Figure 1 shows that a very good signal-to-noise ratio is obtained already at low laser pulse energy in $CD_3CN$, the solvent with the weakest singlet oxygen emission probability. The fit of a convolution of the apparatus function AF($t$) with the a biexponential rise and decay function of eq 2 to the experimental signal yields with high accuracy the preexponential factor $I_{1275}^m$ of eq 3 and $\tau_T$. Recording the same experiment on a much slower time scale yields the $O_2(^1\Delta_g)$ lifetime $\tau_\Delta = 1.20$ ms in $CD_3CN$.

$$I_{1275}^m = c_{1275} n_{1275}^{-2} F_{355} Q_\Delta k_{a-X}^{SOL} E_P \qquad (3)$$

Figure 2 displays the signal $I_{1935}$ of the b → a emission of $O_2(^1\Sigma_g^+)$ sensitized by BRA in $CD_3CN$ in the same experiment.

The half-width of the signal peak of 0.25 ms does not reflect the actual $O_2(^1\Sigma_g^+)$ lifetime but is determined by the high amplification of the detector. The irregular waves forming the baseline of the $O_2(^1\Sigma_g^+)$ signal are caused by acoustic noise and rest as irreproducible underground signal despite the high number of 128 averaged experiments. They represent an important perturbation which still prevents the quantitative determination of $O_2(^1\Sigma_g^+)$ in a more general variety of solvents. Nonetheless, it should be stressed, that Figure 2 shows for the first time a $O_2(^1\Sigma_g^+)$ signal recorded in a highly polar solvent, which can be evaluated quantitatively. The amplitude $INT_{1935}$ is calculated as difference of the maximum signal and the average signal during the last 50 $\mu$s directly before the fast rise of the signal.

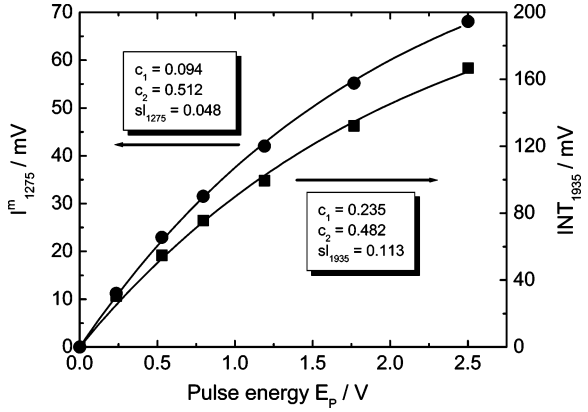


**Figure 3.** Laser pulse energy dependence of the $I_{1275}^m$ and $INT_{1935}$ emission signals of $O_2(^1\Delta_g)$ and $O_2(^1\Sigma_g^+)$ sensitized by BRA in $CD_3CN$ and corresponding fits according to eq 5.

$INT_{1935}$ corresponds to the integral $O_2(^1\Sigma_g^+)$ emission. Therefore, its value is directly proportional to the lifetime $\tau_\Sigma$; see eq 4.

$$INT_{1935} = c_{1935} n_{1935}^{-2} F'_{355} Q_\Sigma k_{b-a}^{SOL} E_P \tau_\Sigma^{SOL} \qquad (4)$$

Figure 3 shows a plot of the signals $I_{1275}^m$ and $INT_{1935}$ sensitized by BRA in $CD_3CN$, which correlate directly with the overall concentrations of $O_2(^1\Delta_g)$ and $O_2(^1\Sigma_g^+)$ with increasing laser pulse energy. Rather smooth but nonlinear dependences on $E_P$ are observed.

In an attempt to evaluate the energy-linear region of both signals, we fitted the experimental data of $I_{1275}^m$ and $INT_{1935}$ by the exponential rise function of eq 5, which is often used in the fitting of TT-absorption measurements. The fits describe the data very well.

$$I = c_1\{1 - \exp(-c_2 E_P)\} \qquad (5)$$

At very low laser pulse energies, i.e., for $E_P \to 0$, both signals are expected to depend linearly on $E_P$. The slope is given by $sl = c_1 \times c_2$ for $E_P \to 0$. Therefore, the slopes $sl_{1275}$ and $sl_{1935}$ are interpreted as energy-normalized signals $I_{1275}^m/E_P$ and $INT_{1935}/E_P$; see eqs 6 and 7.

$$sl_{1275} = I_{1275}^m/E_P = c_{1275} n_{1275}^{-2} F_{355} Q_\Delta k_{a-X}^{SOL} \qquad (6)$$

$$sl_{1935} = INT_{1935}/E_P = c_{1935} n_{1935}^{-2} F'_{355} Q_\Sigma k_{b-a}^{SOL} \tau_\Sigma^{SOL} \qquad (7)$$

$c_{1935}$ and $n_{1935}$ are the apparatus constant and solvent refractive index for 1935 nm. $F'_{355}$ is the geometric factor for in-line observation, and $\tau_\Sigma^{SOL}$ and $k_{b-a}^{SOL}$ are the solvent-dependent $O_2(^1\Sigma_g^+)$ lifetime and rate constant of the radiative b → a transition, respectively. Since the values of $c_{1275}$, $n_{1935}$, $k_{a-X}^{SOL}$, $c_{1935}$, $n_{1935}$, $k_{b-a}^{SOL}$, $F_{355}$, and $F'_{355}$ are constants for a given sample, the ratio $(sl_{1935}/sl_{1275})^S$ obtained with a sensitizer S in the solvent SOL is given by eqs 8 and 9.

$$(sl_{1935}/sl_{1275})^S = c'(Q_\Sigma/Q_\Delta)^S \tau_\Sigma^{SOL} \qquad (8)$$

$$c' = (c_{1935} n_{1275}^2 F'_{355} k_{b-a}^{SOL})/(c_{1275} n_{1935}^2 F_{355} k_{a-X}^{SOL}) \qquad (9)$$

If the ratios $(sl_{1935}/sl_{1275})^S$ and $(sl_{1935}/sl_{1275})^{PHE}$ are determined for sensitizer S and reference PHE in the same solvent, then,

**TABLE 2: Relative Ratios $(Q_\Sigma/Q_\Delta)^S/(Q_\Sigma/Q_\Delta)^{PHE}$ of Quantum Yields of $O_2(^1\Sigma_g^+)$ and Overall $O_2(^1\Delta_g)$ Sensitization Referred to the Reference Sensitizer Phenalenone**

| | $(Q_\Sigma/Q_\Delta)^S/(Q_\Sigma/Q_\Delta)^{PHE}$ | | | | |
|---|---|---|---|---|---|
| sensitizer | TET/B[a] | $CHCl_3$[b] | $CD_3CN$[c] | avg | $\pm\sigma$,[d] % |
| BRA | 0.799 | 0.710 | 0.753 | 0.754 | 8 |
| QUI | 1.555 | 1.416 | 1.467 | 1.479 | 7 |
| ANA | 1.484 | 1.437 | 1.498 | 1.473 | 3 |
| CLA | 1.337 | 1.149 | 1.185 | 1.224 | 11 |

[a] Standard deviation $\sigma$: ±3%. [b] Standard deviation $\sigma$: ±5%. [c] Standard deviation $\sigma$: ±9%. [d] Of average values.

according to eq 10, the calculation of quantum yield ratios $(Q_\Sigma/Q_\Delta)^S$ referred to the quantum yield ratio $(Q_\Sigma/Q_\Delta)^{PHE}$ is possible.

$$(sl_{1935}/sl_{1275})^S/(sl_{1935}/sl_{1275})^{PHE} = (Q_\Sigma/Q_\Delta)^S/(Q_\Sigma/Q_\Delta)^{PHE} \quad (10)$$

These relative ratios have been measured in TET/B, $CHCl_3$, and $CD_3CN$. Table 2 lists the results.

The relative ratios vary by a factor of about 2 from BRA to QUI in TET/B. The comparison with the results in the more polar solvents reveals the same graduation of the data. Therefore, with respect to singlet oxygen sensitization the polarity change of the solvent seems to have no effect on the investigated sensitizers. The most plausible explanation for the solvent polarity independent ratios $(Q_\Sigma/Q_\Delta)^S/(Q_\Sigma/Q_\Delta)^{PHE}$ is the assumption of a solvent independence of the individual ratios $Q_\Sigma/Q_\Delta$ of the sensitizers of Table 2 and of PHE. $Q_\Delta$ data of PHE have been found to be almost unity independent of solvent polarity in a wide range of solvents.[36] Values of $Q_\Delta$ of 0.97, 0.97, and 1.00 have been measured with uncertainties of ±2% in TET, in $CHCl_3$, and in $CH_3CN$. CT interactions are negligibly for PHE in TET/B because of its exceptional large value of $\Delta G_{CET}$; see Table 1. If CT interactions would become effective for PHE in going from nonpolar to polar solvents a lowering of the efficiency $S_\Delta = Q_\Delta/Q_T$ due to the increased CT-induced $O_2(^3\Sigma_g^-)$ formation would be the case but not the observed slight increase of $Q_\Delta$. Therefore, it is reasonable to assume a common quantum yield $Q_\Delta^{PHE} = 0.98$ for these three solvents and for $CD_3CN$ as well. Since both the efficiencies $a$ and $S_\Delta$ are determined for nCT sensitizers by the respective excess energies and thus by $E_T$, which varies only slightly with solvent polarity for planar aromatic $\pi\pi^*$ triplet sensitizers, a constant value for the efficiency $a = Q_\Sigma/Q_T$ can be expected for PHE in these solvents as well. Thus, the previously in TET determined quantum yield $Q_\Sigma^{PHE} = 0.60$ should also be valid in $CHCl_3$ and in $CD_3CN$.[17]

Energy-normalized signals $I^m_{1275}/E_P$ and $INT_{1935}/E_P$ have been measured with sensitizer S and reference PHE under the same experimental conditions in the same solvent. Therefore, eqs 6 and 7 allow via $sl_{1275}^S/sl_{1275}^{PHE} = Q_\Delta^S/Q_\Delta^{PHE}$, $sl_{1935}^S/sl_{1935}^{PHE} = Q_\Sigma^S/Q_\Sigma^{PHE}$, $Q_\Delta^{PHE} = 0.98$, and $Q_\Sigma^{PHE} = 0.60$ the evaluation of single values of $Q_\Delta$ and $Q_\Sigma$ for each investigated sensitizer in TET/B, $CHCl_3$, and $CD_3CN$; see Table 3.

The $Q_\Delta$ and $Q_\Sigma$ data obtained by this evaluation indicate a solvent independence of the quantum yields with exception of CLA, for which both $Q_\Delta$ and $Q_\Sigma$ are by a factor of 4.5 smaller in $CHCl_3$ than in TET/B and in $CD_3CN$. This striking deviation can certainly not be explained by solvent polarity dependent processes but points to additional specific deactivation process of $T_1$ excited CLA in $CHCl_3$ possibly by a photochemical deactivation route.

**$O_2(^1\Sigma_g^+)$ Lifetimes in TET/B, $CHCl_3$, and $CH_3CN$.** In previous work concerning fluorene sensitizers, we determined in a lot of comparative experiments with PHE $O_2(^1\Sigma_g^+)$ lifetimes

**TABLE 3: Quantum Yields $Q_\Sigma$ and $Q_\Delta$ of $O_2(^1\Sigma_g^+)$ and Overall $O_2(^1\Delta_g)$ Sensitization in Solvents of Different Polarity**

| | TET/B | | $CHCl_3$ | | $CD_3CN$ | |
|---|---|---|---|---|---|---|
| sensitizer | $Q_\Sigma$ | $Q_\Delta$ | $Q_\Sigma$ | $Q_\Delta$ | $Q_\Sigma$ | $Q_\Delta$ |
| PHE | 0.60 | 0.98 | 0.60 | 0.98 | 0.60 | 0.98 |
| BA | 0.45[a] | 0.91[b] | 0.42[c] | 0.97[b] | 0.44[e] | 0.95[f] |
| QUI | 0.92[a] | 0.97[b] | 0.80[c] | 0.93[b] | 0.87[e] | 0.97[f] |
| ANA | 0.79[a] | 0.87[b] | 0.76[c] | 0.86[b] | 0.73[e] | 0.79[f] |
| CLA | 0.78[a] | 0.95[b] | 0.16[d] | 0.22[e] | 0.70[e] | 0.96[f] |

[a] Uncertainty: ±5%. [b] Uncertainty: ±3%. [c] Uncertainty: ±6%. [d] Uncertainty: ±15%. [e] Uncertainty: ±10%. [f] Uncertainty: ±4%.

in various batches of $CCl_4$ to $\tau_\Sigma \leq 130$ ns via the time-resolved b → X emission at 765 nm.[23] We simultaneously recorded the integral energy normalized b → a emission $sl_{1935}$ in $CCl_4$ and in TET/B as well. $sl_{1935}$ is directly proportional to the product of the radiative rate constant $k_{b-a}^{SOL}$ of b → a emission and of the $O_2(^1\Sigma_g^+)$ lifetime in the given solvent, see eq 7. Therefore, one obtains from the ratio of $sl_{1935}$ values in TET/B and TET the ratio $(k_{b-a}^{TET/B}\tau_\Sigma^{TET/B})/(k_{b-a}^{TET}\tau_\Sigma^{TET})$. Multiplying this ratio with the corresponding experimental $\tau_\Sigma^{TET}$ values resulted in an average of 1.90 ± 0.12 ns, which was interpreted as $O_2(^1\Sigma_g^+)$ lifetime in TET/B.[23] A more detailed view demonstrates that the solvent dependence of $k_{b-a}^{SOL}$ still has to be considered. The a → X and b → a emissions of $O_2$ are bimolecular collision-induced transitions and depend on the molecular polarizability of the collider.[37] The ratio $k_{a-X}^c/k_{b-a}^c$ of the respective radiative rate constants is a general constant, as was shown theoretically by Minaev and experimentally confirmed by us.[38,39] The radiative rate constant $k_{a-X}^{SOL}$ amounts to 1.17 and 1.50 $s^{-1}$ in TET and in B, respectively.[40] Division by the respective solvent molarities yields second-order rate constants $k_{a-X}^{c,TET}$ and $k_{a-X}^{c,B}$, which can be used to calculate via eq 11 the radiative rate constant $k_{a-X}^{TET/B} = 1.193$ $s^{-1}$ for the solvent mixture TET/B.[40]

$$k_{a-X}^{TET/B} = k_{a-X}^{c,TET}[TET] + k_{a-X}^{c,B}[B] \quad (11)$$

Since $k_{a-X}^{SOL}$ is by 2% larger in TET/B than in TET the same holds true for $k_{b-a}^{SOL}$. If this slight solvent dependence is taken into account, we obtain $\tau_\Sigma^{TET/B} = 1.86 \pm 0.12$ ns. This value compares well with $\tau_\Sigma^{TET/B} = 1.90$ ns, which is obtained for TET/B with the experimental rate constants $k_\Delta^Q = 7.3 \times 10^5$ and $6.6 \times 10^8$ $M^{-1}$ $s^{-1}$ of $O_2(^1\Sigma_g^+)$ quenching by $CCl_4$ and $C_6H_6$.[6]

Using TET/B as reference solvent, it is possible to determine from our experiments $O_2(^1\Sigma_g^+)$ lifetimes in $CHCl_3$ and $CD_3CN$ as well. The ratio of the energy normalized signals $I^m_{1275}/E_P$ and $INT_{1935}/E_P$ of a given sensitizer in a particular solvent is according to eq 8 the product of $c'$, $(Q_\Sigma/Q_\Delta)^S$, and $\tau_\Sigma^{SOL}$. The proportionality constant $c'$ given by eq 9 can well be assumed to be independent of solvent. **(**i**)** The ratio $F'_{355}/F_{355}$ of the geometric factors depends on the absorbance at 355 nm and does not change with solvent for optically matched solutions. **(**ii**)** The refractive index n of solvents decreases in the NIR only weakly with wavelength. For example, the decrease of n amounts to only 1.6% between 1256 and 2000 nm for water.[41] Similarly small changes may be assumed for TET/B, $CHCl_3$, and $CD_3CN$ leading to negligibly small variations of $n_{1275}^2/n_{1935}^2$ with solvent. **(**iii**)** Furthermore, $k_{b-a}^{SOL}/k_{a-X}^{SOL}$ is constant.[38,39] Since the ratio $(Q_\Sigma/Q_\Delta)^S$ can also be assumed solvent independent for nCT sensitzers, see Table 2 and the respective discussion, the ratio of energy normalized signals $(sl_{1935}/sl_{1275})^S$ of a given senstizer recorded with optically matched solutions in the solvents SOL and TET/B should finally correspond

**TABLE 4: Lifetimes of $O_2(^1\Sigma_g^+)$ Determined via eq 12 with Respect to the Reference Solvent TET/B Using the Sensitizers PHE, BRA, QUI, and DQU**

| solvent | $\tau_\Sigma$, ns | $\pm\sigma$,[a] % | $\tau_\Sigma$,[b] ns |
|---|---|---|---|
| $CHCl_3$ | 1.40 | 6 | 1.18 |
| $CD_3CN$ | 0.58 | 8 | 0.61 |
| TET/B | 1.86 | 6 | 1.90 |

[a] Reproducibility. [b] Calculated from experimental quenching rate constants.

directly to the lifetime ratio $\tau_\Sigma^{SOL}/\tau_\Sigma^{TET/B}$; see eq 12.

$$(sl_{1935}/sl_{1275})^{S,SOL}/(sl_{1935}/sl_{1275})^{S,TET/B} = \tau_\Sigma^{SOL}/\tau_\Sigma^{TET/B} \quad (12)$$

The results of these experiments are given in Table 4.

The experimental values of the $O_2(^1\Sigma_g^+)$ lifetimes in $CHCl_3$ and $CD_3CN$ agree very well with respective data calculated from $O_2(^1\Sigma_g^+)$ quenching rate constants. The consistency of these results confirms definitely the assumption of solvent independent ratios $Q_\Sigma/Q_\Delta$ of PHE and of the sensitizers of Table 2.

**Energy Gap Law for the Rate Constants of $O_2(^1\Sigma_g^+)$, $O_2(^1\Delta_g)$, and $O_2(^3\Sigma_g^-)$ Formation in the Absence of CT Interactions.** Equation 13 describes the initial processes of triplet state quenching by $O_2$. $T_1$-excited sensitizer and $O_2(^3\Sigma_g^-)$ form with diffusion-controlled rate constant $k_{diff}$ excited $^{1,3,5}(T_1{}^3\Sigma)$ encounter complexes with multiplicities $m = 1$, 3, and 5. These complexes either dissociate back again with rate constant $k_{-diff}$ or react spin-allowed forward with overall rate constant $k_D$ to yield from $^1(T_1{}^3\Sigma)$ singlet ground-state sensitizer $S_0$ and $O_2(^1\Sigma_g^+)$ or $O_2(^1\Delta_g)$, and from $^3(T_1{}^3\Sigma)$ $S_0$ and $O_2(^3\Sigma_g^-)$; see Scheme 1. The quintet complex $^5(T_1{}^3\Sigma)$ has no direct product channel.

$$T_1 + {}^3\Sigma \underset{k_{-diff}}{\overset{k_{diff}}{\rightleftharpoons}} {}^{1,3,5}(T_1{}^3\Sigma) \xrightarrow{k_D} \quad (13)$$

The $\pi\pi^*$ triplet states of the sensitizers of the present study are completely quenched by $O_2$ in air-saturated solutions. Therefore, the rate constant $k_T^Q$ of $T_1$ state quenching by $O_2$ is calculated by eq 14 from experimentally determined rise times $\tau_T$ of $O_2(^1\Delta_g)$, see Figure 1, and known values of $[O_2]$, see the Experimental Section.

$$k_T^Q = 1/(\tau_T\,[O_2]) \quad (14)$$

The overall rate constant of product formation $k_D$ is calculated by eq 15

$$k_D = k_{-diff}\,k_T^Q/(k_{diff} - k_T^Q) \quad (15)$$

where $k_{diff}$ is taken to be $2.72 \times 10^{10}$ (TET, TET/B),[21−24] $3.48 \times 10^{10}$ ($CHCl_3$),[42] and $4.50 \times 10^{10}$ $M^{-1}$ $s^{-1}$ ($CH_3CN$,[14] $CD_3CN$). The rate constant of backward dissociation is assumed to be $k_{-diff} = k_{diff}/M^{-1}$, with M being the unit molarity.[7,14,21−24] The efficiencies of $O_2(^1\Sigma_g^+)$ and overall $O_2(^1\Delta_g)$ sensitization are $a = Q_\Sigma/Q_T$ and $S_\Delta = Q_\Delta/Q_T$. The single rate constants $k_T{}^{1\Sigma}$, $k_T{}^{1\Delta}$, and $k_T{}^{3\Sigma}$ of $O_2(^1\Sigma_g^+)$, $O_2(^1\Delta_g)$, and $O_2(^3\Sigma_g^-)$ formation can be calculated by eqs 16−18.

$$k_T{}^{1\Sigma} = ak_D \quad (16)$$

$$k_T{}^{1\Delta} = (S_\Delta - a)k_D \quad (17)$$

$$k_T{}^{3\Sigma} = (1 - S_\Delta)k_D \quad (18)$$

Table 5 reports the results of $k_T^Q$, $a$, and $S_\Delta$. Table 6 collects the single rate constants $k_T{}^{1\Sigma}$, $k_T{}^{1\Delta}$, and $k_T{}^{3\Sigma}$ derived from the raw data of Table 5.

The rate constants $k_T^Q$ are much smaller than the values of $k_{diff}$; thus, triplet-state quenching by $O_2$ is not diffusion-controlled. The uncertainties of the rate constants of Table 6 have been evaluated according to the Gaussian law of error propagation. They differ in part strongly and are small for $k_T{}^{1\Sigma}$. The uncertainties of $k_T{}^{1\Delta}$ and $k_T{}^{3\Sigma}$ are mainly determined by the differences $S_\Delta - a$ and $1 - S_\Delta$, respectively, with which they correlate reciprocally. Therefore, the uncertainties become large if theses differences get small. The uncertainties can approximately be estimated to reach factors of 0.3 and 3 for differences smaller than 0.02 and factors of 0.5 and 2 for differences smaller than 0.05. The inspection of the data of Table 6 reveals as remarkable result that, considering the respective uncertainties, for each of the five sensitizers very similar rate constants $k_T{}^{1\Sigma}$, $k_T{}^{1\Delta}$, and $k_T{}^{3\Sigma}$ are found in TET/B, $CHCl_3$, and $CD_3CN$. Two exceptions indicated by bold numbers should be mentioned. **(i)** The $k_T{}^{3\Sigma}$ value of CLA is more than 2 orders of magnitude larger in $CHCl_3$ than in the other two solvents. However, the values of $k_T{}^{1\Sigma}$ and $k_T{}^{1\Delta}$ of CLA do not deviate in $CHCl_3$ since the quantum yields $Q_\Sigma$ and $Q_\Delta$ are correspondingly smaller in that solvent. This result and the extremely large value of $k_T^Q$ for CLA in $CHCl_3$ show unambiguously that an additional deactivation process takes place in $CHCl_3$ for $T_1$ excited CLA, which does not lead to singlet oxygen formation and which could be photochemical. Therefore, the $k_T{}^{3\Sigma}$ value of CLA has to be omitted in the further analysis. **(ii)** The rate constant $k_T{}^{3\Sigma}$ of ANA is not much but significantly larger in $CD_3CN$ than in the two less polar solvents. Such a trend is not observed for the values of $k_T{}^{1\Sigma}$ and $k_T{}^{1\Delta}$ of ANA. We conclude that CT interactions become important for the deactivation channel leading to ground-state oxygen for $T_1$ excited ANA in $CD_3CN$. The CT-induced relative increase of rate constants $k_T{}^{1\Sigma}$, $k_T{}^{1\Delta}$, and $k_T{}^{3\Sigma}$ is generally strongest for $k_T{}^{3\Sigma}$, since these rate constants are in the absence of CT interactions the smallest ones, see Table 6. Thus, the value of $k_T{}^{3\Sigma}$ of ANA has already CT contributions in $CD_3CN$ and will be disregarded in the further discussion. In fact, ANA has by far the smallest value of $\Delta G_{CET}$ of the sensitizers of Table 1.

It was previously shown that the multiplicity-normalized rate constants $k_T{}^P/m$ ($= k_T{}^{1\Sigma}/1$, $k_T{}^{1\Delta}/1$, and $k_T{}^{3\Sigma}/3$) depend in a common way on excess energies $\Delta E$ of the respective product channels for $T_1(\pi\pi^*)$ nCT sensitizers in TET.[21−24] These results led to the conclusion that the formation of $O_2(^1\Sigma_g^+)$, $O_2(^1\Delta_g)$, and $O_2(^3\Sigma_g^-)$ proceeds from $^1(T_1{}^3\Sigma)$ and $^3(T_1{}^3\Sigma)$ nCT complexes being in a fully established fast intersystem crossing (ISC) equilibrium; see Scheme 1. Internal conversion (IC) occurs by slower rate determining steps from $^{1,3}(T_1{}^3\Sigma)$ nCT complexes to the lower-lying nCT complexes $^1(S_0{}^1\Sigma)$, $^1(S_0{}^1\Delta)$, and $^3(S_0{}^3\Sigma)$ which dissociate to the respective products. The IC of the $^{1,3}(T_1{}^3\Sigma)$ nCT complexes is ruled in TET by the empirical energy gap relation $\log(k_{\Delta E}{}^P/m) = f(\Delta E)$ of eq 19.

$$\log(k_{\Delta E}{}^P/m/s^{-1}) = 9.05 + (9 \times 10^{-3}\Delta E) - (1.15 \times 10^{-4}\Delta E^2) + (1.15 \times 10^{-7}\Delta E^3) + (9.1 \times 10^{-11}\Delta E^4) \quad (19)$$

As soon as CT interactions become important in $^{1,3}(T_1{}^3\Sigma)$ excited complexes the experimental rate constants $k_T{}^P/m$ deviate significantly from this polynomial to larger values. In this case, an additional second deactivation path is opened which competes with the IC of the primarily formed $^{1,3}(T_1{}^3\Sigma)$ nCT complexes

**TABLE 5: Photophysical Data of $\pi\pi^*$ Triplet Sensitizers Relevant to $T_1$ State Quenching by $O_2$ in Solvents of Different Polarity**

| | TET/B | | | $CHCl_3$ | | | $CD_3CN$ | | |
|---|---|---|---|---|---|---|---|---|---|
| sensitizer | $a$ | $S_\Delta$ | $k_T^Q/10^9$, $M^{-1}$ $s^{-1}$ | $a$ | $S_\Delta$ | $k_T^Q/10^9$, $M^{-1}$ $s^{-1}$ | $a$ | $S_\Delta$ | $k_T^Q/10^9$, $M^{-1}$ $s^{-1}$ |
| PHE | 0.600 | 0.980 | 2.11[a] | 0.600 | 0.980 | 2.02[b] | 0.600 | 0.980 | 2.00[b] |
| BRA | 0.451[d] | 0.923[e] | 2.67[a] | 0.424[f] | 0.976[e] | 2.71[b] | 0.446[f] | 0.961[i] | 2.67[b] |
| QUI | 0.929[d] | 0.976[e] | 0.72[a] | 0.811[f] | 0.936[e] | 0.80[b] | 0.882[f] | 0.976[i] | 0.74[b] |
| ANA | 0.881[d] | 0.970[e] | 1.29[a] | 0.841[f] | 0.956[e] | 1.25[b] | 0.806[f] | 0.878[i] | 1.63[b] |
| CLA | 0.796[d] | 0.973[e] | 1.20[a] | 0.160[g] | 0.226[h] | 6.30[c] | 0.711[f] | 0.983[i] | 1.15[b] |

[a] Uncertainty neglecting the error of the solubilities of $O_2$: ±2%. [b] Uncertainty neglecting the error of the solubilities of $O_2$: ±4%. [c] Uncertainty neglecting the error of the solubilities of $O_2$: ±7%. [d] Uncertainties: ±5%. [e] Uncertainties: ±3%. [f] Uncertainties: ±6%. [g] Uncertainties: ±15%. [h] Uncertainties: ±10%. [i] Uncertainties: ±4%.

**TABLE 6: Rate Constants $k_T^{1\Sigma}$, $k_T^{1\Delta}$, and $k_T^{3\Sigma}$ of Competitive Formation of $O_2(^1\Sigma_g^+)$, $O_2(^1\Delta_g)$, and $O_2(^3\Sigma_g^-)$ in $T_1$ State Quenching by $O_2$ (All Values Are Divided by $10^9$)**

| | TET/B | | | $CHCl_3$ | | | $CD_3CN$ | | |
|---|---|---|---|---|---|---|---|---|---|
| sensitizer | $k_T^{1\Sigma}$, $s^{-1}$ | $k_T^{1\Delta}$, $s^{-1}$ | $k_T^{3\Sigma}$, $s^{-1}$ | $k_T^{1\Sigma}$, $s^{-1}$ | $k_T^{1\Delta}$, $s^{-1}$ | $k_T^{3\Sigma}$, $s^{-1}$ | $k_T^{1\Sigma}$, $s^{-1}$ | $k_T^{1\Delta}$, $s^{-1}$ | $k_T^{3\Sigma}$, $s^{-1}$ |
| PHE | 1.33[a] | 0.84[c] | 0.04[i] | 1.28[f] | 0.81[c] | 0.04[i] | 1.36[f] | 0.86[c] | $0.04_5$[i] |
| BA | 1.34[b] | 1.40[c] | 0.23[e] | 1.24[c] | 1.61[c] | 0.07[i] | 1.35[c] | 1.56[c] | 0.12[i] |
| QUI | 0.69[b] | $0.03_5$[i] | 0.02[i] | 0.66[c] | 0.10[d] | 0.05[d] | 0.70[c] | 0.07[h] | 0.02[i] |
| ANA | 1.19[b] | 0.12[d] | 0.04[i] | 1.12[c] | 0.15[d] | 0.06[h] | 1.47[c] | 0.13[h] | **0.22**[e] |
| CLA | 1.00[b] | 0.22[e] | 0.03[i] | 1.21[g] | 0.50[d] | **5.88**[c] | 0.87[c] | $0.33_5$[g] | 0.02 [j] |

[a] Uncertainty neglecting the error of the solubilities of $O_2$: ±3%. [b] Uncertainty neglecting the error of the solubilities of $O_2$: ±5%. [c] Uncertainty neglecting the error of the solubilities of $O_2$: ±10%. [d] Uncertainty neglecting the error of the solubilities of $O_2$: ±50%. [e] Uncertainty neglecting the error of the solubilities of $O_2$: ±30%. [f] Uncertainty neglecting the error of the solubilities of $O_2$: ±4%. [g] Uncertainty neglecting the error of the solubilities of $O_2$: ±20%. [h] Uncertainty neglecting the error of the solubilities of $O_2$: ±70%. [i] By factors of 0.5 and 2%. [j] By factors of 0.3 and 3%.

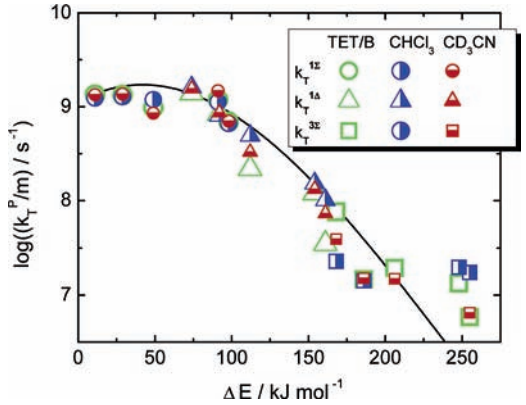


**Figure 4.** Dependence of the multiplicity normalized rate constants of $O_2(^1\Sigma_g^+)$, $O_2(^1\Delta_g)$, and $O_2(^3\Sigma_g^-)$ formation on the respective excess energies $\Delta E$ for the sensitizers of Table 6 in solvents of different polarity. The solid line represents the energy gap relation of eq 19.

and leads via $^{1,3}(T_1{}^3\Sigma)$ exciplexes with partial CT character (= CT complexes) also to formation of $O_2(^1\Sigma_g^+)$, $O_2(^1\Delta_g)$, and $O_2(^3\Sigma_g^-)$; see the dotted lines of Scheme 1.

The lack of any solvent polarity effect on the rate constants $k_T^{1\Sigma}$, $k_T^{1\Delta}$ and $k_T^{3\Sigma}$ indicates that $T_1(\pi\pi^*)$ deactivation by $O_2$ occurs for the sensitizers of Table 6 with the above-mentioned restriction without CT interactions, i.e., via the nCT channel in TET/B, $CHCl_3$, and $CD_3CN$. The investigated sensitizers cover a wide range of triplet energies. Therefore, they allow to test whether the energy gap relation of eq 19 also describes the excess energy dependence of the $\log(k_T^P/m)$ values in polar solvents. Figure 4 plots the $\log(k_T^P/m)$ of Table 6 as a function of $\Delta E$ in addition to the polynomial $\log(k_{\Delta E}^P/m) = f(\Delta E)$.

The experimental data follow rather closely the previously derived energy gap relation. It appears as if there could be some structure or modulation in the $\Delta E$ dependence of the data. However, considering the in part significant experimental uncertainties given in Table 6, it has to be stated that the principal excess energy dependence of the $\log(k_T^P/m)$ data is well described for nonpolar and strongly polar solvents as well. Thus, eq 19, $\log(k_{\Delta E}^P/m) = f(\Delta E)$, is more than a simple energy gap relation. It represents a general energy gap law for the rate constants of the IC processes $^1(T_1{}^3\Sigma) \rightarrow {}^1(S_0{}^1\Sigma)$, $^1(T_1{}^3\Sigma) \rightarrow {}^1(S_0{}^1\Delta)$, and $^1(T_1{}^3\Sigma) \rightarrow {}^3(S_0{}^3\Sigma)$ in the absence of CT interactions, i.e., of the IC of excited $^{1,3}(T_1{}^3\Sigma)$ encounter complexes.

Equation 20 was derived for the rate constant $k_{IC}$ of a weakly bound complex of an excited sensitizer molecule and $O_2$ by Kawaoka et al.[43]

$$k_{IC} = (4\pi^2/h)\rho(\Delta E)F(\Delta E)\beta^2 \qquad (20)$$

Here, $\rho(\Delta E)$ is the density of final states which are nearly degenerate with the initial state, $F(\Delta E)$ is the Franck−Condon factor, and $\beta$ is the electronic coupling matrix element. The product $F'(\Delta E) = \rho(\Delta E)F(\Delta E)$ is the Franck−Condon weighted density of states and can be calculated from the shape of the corresponding emission spectra.[44−48] $F'(\Delta E)$ generally decreases with increasing $\Delta E$ at higher excess energies, which qualitatively explains the decrease of the rate constants $k_{IC}$ with $\Delta E$. It is important to note that the dependence of $\log(k_{\Delta E}^P/m)$ on $\Delta E$ given by eq 19 is very similar in shape to the energy gap law found by Siebrand and co-workers for the rate constants of radiationless deactivation of excited aromatic compounds, molecules with potential energy curves with deep minima and small anharmonicity.[44−46] However, the curve $\log(k_{\Delta E}^P/m) = f(\Delta E)$ declines much weaker in the region of high excess energies than Siebrand's energy gap law. This difference is consistently explained by the only weak binding interactions of excited $^{1,3}(T_1{}^3\Sigma)$ encounter complexes of nCT sensitizers corresponding to shallow potential minima with large anharmonicity.

The findings concerning the triplet sensitization of singlet oxygen are excellently complemented by the results of a recent analysis of the likewise not diffusion-controlled rate constants of the quenching of $O_2(^1\Delta_g)$ by 28 carotenoids.[49,50] It could be shown that CT interactions are negligible and that the excess

energy dependence of the rate constants of electronic energy transfer according to eq 21 is quantitatively described by eq 19.

$$O_2(^1\Delta_g) + S_0 \rightarrow O_2(^3\Sigma_g^-) + T_1 \qquad (21)$$

Actually, it was only necessary to consider the differing spin-statistical factors of triplet sensitization of $O_2(^1\Delta_g)$ and of its formal back reaction, the $O_2(^1\Delta_g)$ quenching by singlet ground-state molecules. Moreover, eq 19, originally derived from experiments in the nonpolar TET, satisfied rate constants of $O_2(^1\Delta_g)$ quenching determined in the highly polar solvent mixture $C_2H_5OH/CHCl_3/D_2O$.

## Conclusion

If triplet-state quenching by $O_2$ occurs without charge-transfer interactions, the rate constants of $O_2(^1\Sigma_g^+)$, $O_2(^1\Delta_g)$, and $O_2(^3\Sigma_g^-)$ formation follow a common dependence on the respective excess energies, independent of solvent polarity. This empirical energy gap relation also describes the rate constants of the quenching of $O_2(^1\Delta_g)$ by carotenoids, formally being the back reaction of singlet oxygen sensitization. Therefore, eq 19 represents a generally valid energy gap law for the rate constants of electronic energy transfer to and from $O_2$ for the absence of CT interactions

Meanwhile, a very valuable database has been acquired on the electronic energy transfer to and from $O_2$.[21−24,49,50] These energy transfer processes have only insufficiently been studied theoretically in the past, probably because of the previously weak database and perhaps because of the difficulties in the theoretical treatment of electronic energy transfer processes with $O_2$ with its open shell electronic structure. Since, however, theoretical and computational chemistry have strongly developed, it is hoped that this article could stimulate a complementary theoretical study.

**Acknowledgment.** Financial support by the Deutsche Forschungsgemeinschaft and the Adolf Messer Stiftung is gratefully acknowledged.

## References and Notes

(1) Schweitzer, C.; Schmidt, R. *Chem. Rev.* **2003**, *103*, 1685.
(2) Griesbeck, A. G.; El-Idreesy, T. T.; Bartoschek, A. *Pure Appl. Chem.* **2005**, *77*, 1059.
(3) Skovsen E.; Snyder J. W.; Lambert J. D. C.; Ogilby, P. R. *J. Phys. Chem. B* **2005**, *109*, 8570.
(4) Niedre, M. J.; Secord, A. J.; Patterson, M. S.; Wilson, B. C. *Cancer Res.* **2003**, *63*, 7986.
(5) Schmidt, R.; Bodesheim, M. *Chem. Phys. Lett.* **1993**, *213*, 111.
(6) Schmidt, R.; Bodesheim, M. *J. Phys. Chem. A* **1998**, *102*, 4769.
(7) Gijzeman, O. L. J.; Kaufman, F.; Porter, G. *J. Chem. Soc., Faraday Trans. 2* **1973**, *69*, 708.
(8) Garner, A.; Wilkinson, F. *Chem. Phys. Lett.* **1977**, *45*, 432.
(9) Cebul, F. A.; Kirk, K. A.; Lupo, D. W.; Pittenger, L. M.; Schuh, M. D.; Williams, I. F.; Winston, G. C. *J. Am. Chem. Soc.*, **1980**, *102*, 5656.
(10) Smith, G. *J. Chem. Soc., Faraday Trans. 2* **1982**, *78*, 769.
(11) McGarvey, D. J.; Szekeres, P. G.; Wilkinson, F. *Chem. Phys. Lett.* **1992**, *199*, 314.
(12) Wilkinson, F.; McGarvey, D. J.; Olea, A. F. *J. Phys. Chem.* **1994**, *98*, 3762.
(13) Wilkinson, F.; Abdel-Shafi, A. A. *J. Phys. Chem. A* **1997**, *101*, 5509.
(14) Wilkinson, F.; Abdel-Shafi, A. A. *J. Phys. Chem. A* **1999**, *103*, 5425.
(15) Grewer, C.; Brauer, H.-D. *J. Phys. Chem.* **1994**, *98*, 4230.
(16) Darmanyan, A. P.; Lee, W.; Jenks, W. S. *J. Phys. Chem. A* **1999**, *103*, 2705.
(17) Bodesheim, M.; Schütz, M.; Schmidt, R. *Chem. Phys. Lett.* **1994**, *221*, 7.
(18) Schmidt, R.; Bodesheim, M. *J. Phys. Chem.* **1994**, *98*, 2874.
(19) Chou, P. T.; Wei, G. T.; Lin, C. H.; Wei, C. Y.; Chang, C. H. *J. Am. Chem. Soc.* **1996**, *118*, 3031.
(20) Losev, A. P.; Bachilo, S. M.; Nichiporovich, I. N. *J. Appl. Spectrosc.* **1998**, *65*, 1.
(21) Schmidt, R.; Shafii, F.; Schweitzer, C.; Abdel-Shafi, A. A.; Wilkinson, F. *J. Phys. Chem. A* **2001**, *105*, 1811.
(22) Schmidt, R.; Shafii, F. *J. Phys. Chem. A* **2001**, *105*, 8871.
(23) Mehrdad, Z.; Noll, A.; Grabner, E.-W.; Schmidt, R. *Photochem. Photobiol. Sci.* **2002**, *1*, 263.
(24) Schweitzer, C.; Mehrdad, Z.; Noll, A.; Grabner, E.-W.; Schmidt, R. *J. Phys. Chem. A* **2003**, *107*, 2192.
(25) Schmidt, R. *Photochem. Photobiol. Sci.* **2005**, *4*, 481.
(26) Rehm, D.; Weller, A. *Isr. J. Chem.* **1970**, *8*, 259.
(27) Mattes, S. L.; Farid, S. In *Organic Photochemistry*; Padwa, A., Ed.; Marcel Dekker: New York, 1983.
(28) Shafii, F.; Schmidt, R. *J. Phys. Chem. A* **2001**, *105*, 1805.
(29) Yu, W.; Pellegrino, F.; Grant, M.; Alfano, R. R. *J. Chem. Phys.* **1977**, *67*, 1766.
(30) Murov, L. S.; Carmichael, I.; Hug, G. L. *Handbook of Photochemistry*, 2nd ed.; Marcel Dekker: New York, 1993.
(31) Clark, W. D. K.; Steel, S. *J. Am. Chem. Soc.* **1971**, *93*, 6347.
(32) Franco, C.; Olmsted, J. *Talanta* **1990**, *37*, 905.
(33) Oliveros, E.; Murasecco-Suardi, P.; Aminian-Saghafi, T.; Braun, A. M.; Hansen, H.-J. *Helv. Chim. Acta* **1991**, *74*, 79.
(34) Hamanoue, K.; Hidaka, T.; Nakayama, T.; Teranishi, H.; Sumitani, M.; Yoshihara, K. *Bull. Chem. Soc. Jpn* **1983**, *56*, 1851.
(35) Lamola, A. A.; Hammond, G. S. *J. Chem. Phys.* **1965**, *43*, 2129.
(36) Schmidt, R.; Tanielian, C.; Dunsbach, R.; Wolff, C. *J. Photochem. Photobiol. A: Chem.* **1994**, *79*, 11.
(37) Schmidt, R.; Bodesheim, M. *J. Phys. Chem.* **1995**, *99*, 15919.
(38) Minaev, B. F.; Lunell, S.; Kobzev, G. I. *THEOCHEM* **1993**, *284*, 1.
(39) Hild, M.; Schmidt, R. *J. Phys. Chem. A* **1999**, *103*, 6091.
(40) Schmidt, R.; Shafii, F.; Hild, M. *J. Phys. Chem. A* **1999**, *103*, 2599.
(41) Lax, E., Ed. *D'Ans Lax, Taschenbuch für Chemiker und Physiker Vol. 1*; Springer-Verlag: Berlin, 1967; p 628.
(42) Interpolated value using the viscosities $\eta$ of 0.341 ($CH_3CN$), 0.898 ($CHCl_3$), and 0.536 cP (TET) from ref 30, p 208, assuming $k_{diff} \sim \eta^{-1}$.
(43) Kawaoka, K.; Khan, A. U.; Kearns, D. R. *J. Chem. Phys.* **1967**, *46*, 1842.
(44) Siebrand, W.; Williams, D. F. *J. Chem. Phys.* **1967**, *46*, 403.
(45) Siebrand, W. *J. Chem. Phys.* **1967**, *47*, 2411.
(46) Siebrand, W.; Williams, D. F. *J. Chem. Phys.* **1968**, *49*, 1860.
(47) Gould, I. R.; Noukakis, D.; Gomez-Jahn, L.; Young, R. H.; Goodman J. L.; Farid, S. *Chem. Phys.* **1993**, *176*, 439.
(48) Gould, I. R.; Farid, S.; Young, R. H. *J. Photochem. Photobiol. A: Chem.* **1992**, *65*, 133.
(49) Schmidt, R. *J. Phys. Chem. A* **2004**, *108*, 5509.
(50) Baltschun, D.; Beutner, S.; Briviba, K.; Martin, H.-D.; Paust, J.; Peters, M.; Röver, S.; Sies, H.; Stahl, W.; Steigel, A.; Stenhorst, F. *Liebigs Ann./Recueil* **1997**, 1887.